TOPICAL REVIEW — Quantum information

Quantum metrology*

Xiang Guo-Yong(项国勇) and Guo Guang-Can(郭光灿)†

Key Laboratory of Quantum Information, University of Science and Technology of China, Hefei 230026, China

(Received 30 September 2013)

The statistical error is ineluctable in any measurement. Quantum techniques, especially with the development of quantum information, can help us squeeze the statistical error and enhance the precision of measurement. In a quantum system, there are some quantum parameters, such as the quantum state, quantum operator, and quantum dimension, which have no classical counterparts. So quantum metrology deals with not only the traditional parameters, but also the quantum parameters. Quantum metrology includes two important parts: measuring the physical parameters with a precision beating the classical physics limit and measuring the quantum parameters precisely. In this review, we will introduce how quantum characters (e.g., squeezed state and quantum entanglement) yield a higher precision, what the research areas are scientists most interesting in, and what the development status of quantum metrology and its perspectives are.

Keywords: quantum entangled state, phase estimation, quantum imaging, quantum tomography

PACS: 06.20.–f, 42.25.Hz, 42.50.Dv, 42.65.Lm **DOI:** 10.1088/1674-1056/22/11/110601

1. Introduction

The progress of human civilization, in some sense, is a progress of improving the precision of measurement. From the unit defined by the lengthes of foot, hand, step, etc. to that with vernier calipers, microscope, laser ranging device, etc., the measurement precision is improved greatly, and the quality of people's life has greatly improved at the same time. Precision measurement is not only important to demonstrate physical theories, but also helpful to propose new theories and new techniques. The measurement of relative displacement has been improved to the sub-wavelength level, which has been used in cosmology, nano-science, medical science, and so on.

Because of the limitation of classical physics (eg., shot noise), the precision of classical metrology can only reach the limit of classical physics, the standard quantum limit (SQL). A new method is needed to improve the precision and beat the SQL. With the development of quantum mechanics, especially quantum information, more and more works are focusing on the preparation, control, and measurement of quantum entangled states, and great improvements have been achieved. Recently, quantum states, especially quantum entangled states, together with the techniques of classical metrology and the character of quantum mechanics, are used to improve the precision of measurement, which can beat the standard quantum limit $1/\sqrt{N}$ (N is the resource, eg., number of particles). If we estimate (or measure) a phase with some quantum states, squeezed states, and quantum entangled states, the precision could reach the limit of quantum mechanics, the Heisenberg limit $1/N$.

Firstly, we will introduce how squeezed states and quantum entangled states can enhance the precision of measurement.

1.1. Squeezed states of light

In quantum mechanics, a coherent optical field is a coherent state whose uncertainty is equally distributed to X and P, see Fig. 1(a). The Heisenberg uncertainty relation between X and P is

$$\Delta X \cdot \Delta P \geq \hbar/2,$$

and for coherent states, $\Delta X \cdot \Delta P = \hbar/2$. If we add a phase shift $\delta\phi$ to a coherent state, the vector is rotated by $\delta\phi$ in the phase space as shown in Fig. 1(a). If we measure the phase shift between two coherent states, the fluctuation limits the precision of phase measurement. Here, the fluctuation is the vacuum noise, and we can not reduce the vacuum noise to improve the precision with the methods of classical physics. This limit is the shot noise limit. Quantum mechanics can help us squeeze P as shown in Fig. 1(b), and the new state is a squeezed state, which is a quantum light field. The minimum phase shift that can be measured in Fig. 1(a) is the phase difference when two coherent states can just be distinguished, which is limited by the vacuum noise. And it is easier to find that the squeezed state can help to minimize this phase shift (Fig. 1(b)). So the precision of measuring a phase shift can be improved and the shot noise limit is beaten by using the squeezed state.

*Project supported by the National Basic Research Program of China (Grant Nos. 2011CBA00200 and 2011CB9211200), the National Natural Science Foundation of China (Grant Nos. 61108009 and 61222504), the Anhui Provincial Natural Science Foundation, China (Grant No. 1208085QA08), and the Ph. D. Program Foundation of Ministry of Education of China (Grant No. 20113402120017).

†Corresponding author. E-mail: gcguo@ustc.edu.cn

© 2013 Chinese Physical Society and IOP Publishing Ltd

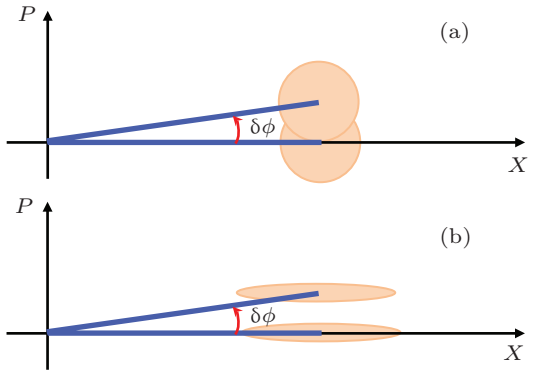


Fig. 1. Precision of phase estimation can be improved by the squeezed state.

1.2. Quantum entangled state

In 1935, Albert Einstein, Boris Podolsky, and Nathan Rosen proposed a gedanken experiment with which they attempted to show that quantum mechanical theory was incomplete, which is the EPR paradox (Einstein–Podolsky–Rosen paradox).[1] In their work, the counterintuitive predictions of quantum mechanics about strongly correlated systems were first discussed. They proposed the entangled state, although they have not coin the word entanglement, nor did they generalize the special properties of the state they considered.

The quantum entangled state was proposed to demonstrate "the quantum-mechanical description of physical reality given by wave functions is not complete", however the quantum entangled states have been used to demonstrate that quantum mechanics can violate the Bell inequality based on the principle of locality, which is not consistent with the hidden variables interpretation of quantum theory that EPR purported to establish. With the development of quantum information, the entangled states have been broadly used in every field of quantum information, such as, quantum dense coding, quantum teleportation, quantum computation, and quantum network. Recently, it is found that the entangled states can be used to improve the precision of measurement. The standard quantum limit can be beaten by using some entangled states, and it will lead to the Heisenberg limit.

For example, if we use the following entangled state:

$$\frac{1}{\sqrt{2}}(\underbrace{|0\rangle\cdots|0\rangle}_{N\text{ times}}+\underbrace{|1\rangle\cdots|1\rangle}_{N\text{ times}}), \tag{1}$$

where N is the number of particles. The state is an N-particle Schrödinger cat state. When we add a phase ϕ to mode $|1\rangle$, there will be a $N\phi$ phase difference between the two modes of the state

$$\frac{1}{\sqrt{2}}(\underbrace{|0\rangle\cdots|0\rangle}_{N\text{ times}}+\mathrm{e}^{\mathrm{i}N\phi}\underbrace{|1\rangle\cdots|1\rangle}_{N\text{ times}}). \tag{2}$$

After a proper quantum measurement, we can obtain a curve with the oscillating period of $2\pi/N$. As shown in Fig. 2 for $N=4$, the red one is the result for the quantum entangled state and the black one is the result for the classical state. It is easy to show that the quantum entangled state can improve the precision to $1/N$, which is $\sqrt{N}$ enhancement over the precision by the classical state.[2]

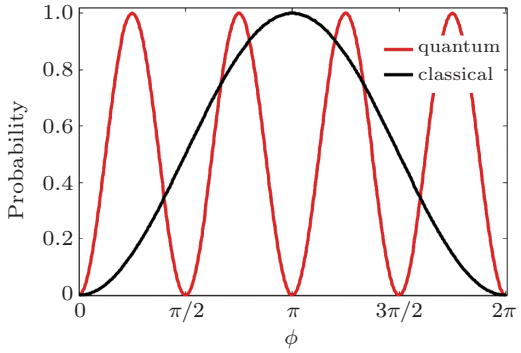


Fig. 2. Quantum phase estimation with Schrödinger cat state and classical state. The red curve is the result with four-particle cat state, and the black one is the result with classical state.

As we know, there are some special parameters for quantum mechanics, such as fidelity, purity, and dimensions of quantum states and quantum systems. So comparing to the classical metrology, quantum metrology not only aims to use quantum resources to develop new methods to measure classical parameters with higher precision than that in classical methods, but also aims to measure quantum parameters with high accuracy.

Quantum metrology is the interdiscipline of quantum mechanics and classical metrology. With improving ability to control quantum systems, new techniques will be developed from quantum metrology, and it will be broadly used.

2. Development status of quantum metrology

Now quantum metrology is mostly focusing on quantum phase estimation, quantum imaging, the measurement of quantum state and process, and so on.

2.1. Quantum phase estimation

The quantum phase estimation aims to measure or estimate any phase or phase shift with a precision beating the standard quantum limit (or shot-noise limit) by using nonclassical optical fields. Suppose that there are N photons and we want to measure a phase by using these photons. If the N photons are in a classical state, the precision will be limited by the shot-noise limit because of the shot noise fluctuation of the photons; if the N photons have a quantum correlation among them, the precision could be enhanced and the shot noise limit would be beaten. In 1980s, scientists have used squeezed states to estimate an optical phase with a measurement precision beyond the shot-noise limit.[3] After that, theorists were trying to develop new methods to realize optimal measurements by using general quantum states, but the measurements could not

be realized because of the experimental problem for a long time. Recently, with the preparation of three-photon and four-photon NOON states, scientists renewed the interest in quantum phase estimation.

In 2007, Nagata *et al.*[4] demonstrated the super resolution of phase estimation by using a four-photon NOON state and the post-selection measurement. They prepared a four-photon Holland–Burnett[5] state after the first 50 : 50 beam splitter with input $|2\rangle_a|2\rangle_b$, a phase shift (PS) was applied to mode d, and $|3\rangle_e|1\rangle_f$ or $|1\rangle_e|3\rangle_f$ was detected after the second beam splitter, see Fig. 3. The probability of detecting three photons in output e and one photon in f was $P_{3e1f} = \frac{3}{8}(1 - \cos 4\phi)/2$, which shows the phase super resolution. They observed the four-photon fringe with $91 \pm 6\%$ (see Fig. 4), which is greater than threshold $V_{th} = \sqrt{2/3} \approx 81.6\%$.[4] In the following year, Sun[6] obtained a higher precision by detecting the $|2\rangle_e|2\rangle_f$ output in Ref. [4]. Most recently, Xiang[7] investigated the achievable phase sensitivity of the simple and efficient single interference fringe detection technique. They showed that the maximally-entangled NOON state does not achieve the optimal phase sensitivity when $N > 4$. Rather, they showed that the Holland–Burnett state is optimal. And they experimentally demonstrated this enhanced sensitivity using a single photon-counted fringe of the six-photon Holland–Burnett state. Specifically, their single-fringe six-photon measurement achieved a phase variance three times below the SNL.

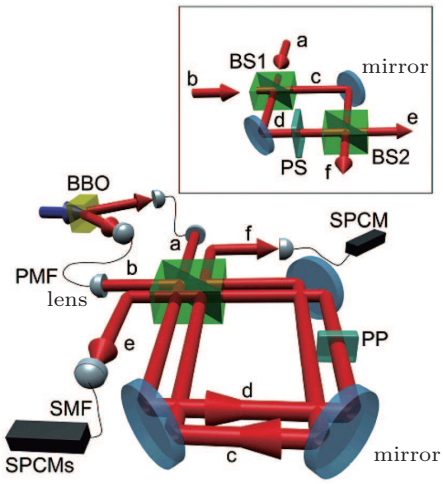


Fig. 3. An optical interferometer for beating the SQL.[4]

The work above is to estimate a phase shift or fluctuation, however in some case, we want to know what the phase is, i.e., measuring a totally unknown phase. In 2007, Higgins *et al.*[8] measured an unknown phase with a precision beating the standard quantum limit by using single-photon Fock states, adaptive measurement, and feedback control. They replaced the entangled input states with multiple applications of the phase shift on unentangled single-photon states and generalized Kitaev's phase estimation algorithm using the adaptive measurement theory to achieve a standard deviation scaling at the Heisenberg limit. Figure 5 shows the quantum circuit diagrams of Kitaev's phase estimation algorithm and its generalization, and figure 6 is the conceptual diagram of the algorithm's implementation as a Mach–Zehnder interferometer. For the largest number of resources used ($N = 378$), they estimated an unknown phase with a variance more than 10 dB below the standard quantum limit; achieving this variance would require more than 4000 resources using the standard interferometry, as shown in Fig. 7. Their results represent a drastic reduction in the complexity of achieving quantum-enhanced measurement precision.

Theoretically, the precision of their method could approach the Heisenberg limit. However in the experiment, because of the multi-pass of the photons, it needs harsh terms of bandwidth when N is large. To overcome this problem, Xiang *et al.*[9] changed the multi-pass into a single pass by optimally utilizing the available entangled photon states, obtained by post-selection.[4,10] They provided a powerful and general bottom-up approach to the *ab initio* estimation of an optical

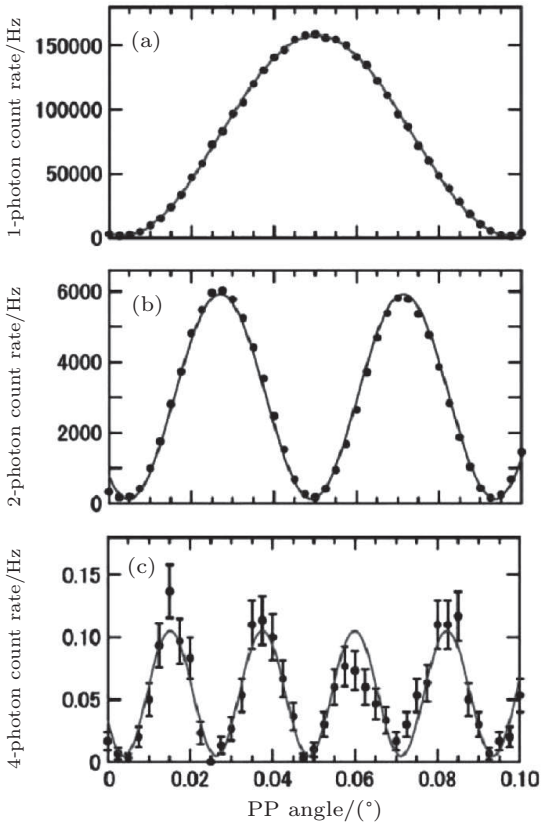


Fig. 4. Beating the standard quantum limit with four entangled photons. (a) Single-photon count rate in mode e as a function of phase plate (PP) angle with single photon input $|10\rangle_{ab}$. (b) Two-photon count rate in modes e and f for input state $|11\rangle_{ab}$. (c) Four-photon count rate with three photons in mode e and one photon in mode f for input state $|22\rangle_{ab}$. Accumulation times for one data point were (a) 1 s, (b) 300 s, and (c) 300 s.[4]

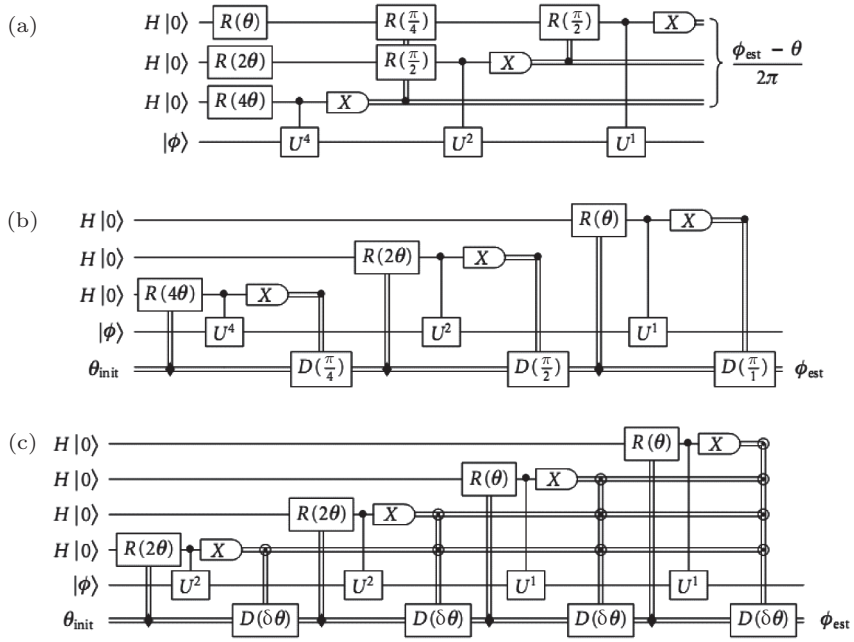


Fig. 5. Quantum circuit diagrams of Kitaev's phase estimation algorithm and our generalization. (a) Kitaev's algorithm with the inverse quantum Fourier transform implemented with measurement and classical feedback and a random initial phase estimate θ. In grneral , $K+1$ qubits yield $K+1$ binary digits of precision; here $K=2$. (b) As in Kitaev's algorithm, but here we implement θ (now called $\theta_{\rm init}$) and the feedback operations by coupling the qubits to a commom element, the feedback phase θ (the lowest rail). (c) Generalization of the circuit to include $M \geq 1$ qubits for each binary digit; here $K=1$ and $M=2$.[8]

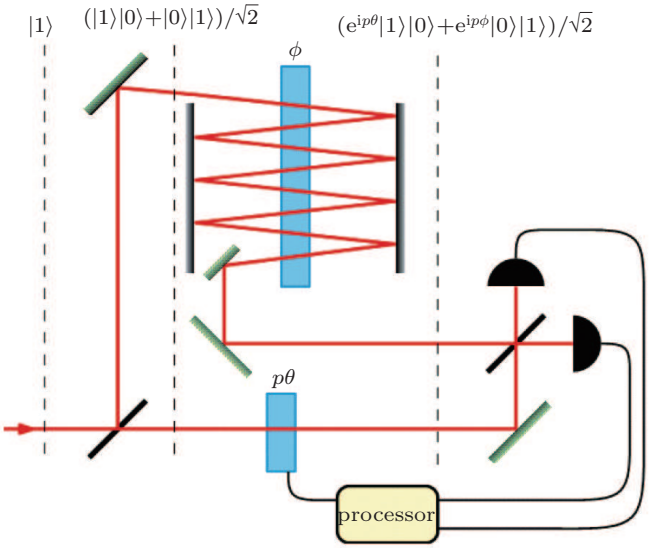


Fig. 6. Conceptual diagram of the algorithm's implementation as a Mach–Zehnder interferometer. This is equivalent to the scheme in Fig. 5(c). Photon-number quantum states are shown at key points. The first beam splitter implements the Hadamard operation on incident photons. The large phase-shift element is configured to implement a $p\phi$ phase shift on logical $|1\rangle$ states, with p adjustable ($p=8$ shown). The small phase-shift element implements the adjustable $p\theta$ phase shift on logical $|0\rangle$ states. The final beam splitter and single photon detectors implement the σ_x measurement, which determines, via the processor, how to adjust θ before the next photon input.[8]

phase $\phi \in [0, 2\pi)$ by using the Bayesian analysis and optimal adaptive feedback to make the best use of available multiphoton states. That is the first demonstration of sub-SNL measurement of a totally random phase using entangled states, which can potentially achieve a high bandwidth in quantum-enhanced phase measurements with a wide range of metrological applications.[9]

Quantum phase estimation has been used to detect the concentrations of some liquids[11] and the gravitational wave.[12] Now, scientists start to consider the following problems. How can we enhance the precision of phase estimation and measurement in the case of photon lossess and unperfect detect efficiency in real situation?[13–15] Can we beat the Heisenberg limit?[16] How can we track a randomly varying optical phase?[17]

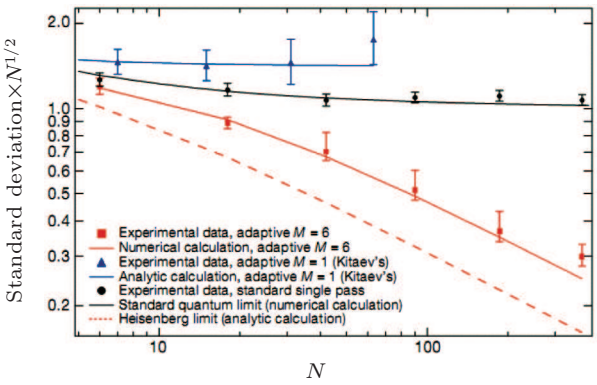


Fig. 7. Standard deviations of distributions of phase estimates for varying numbers of resources N. We compare theoretical predictions (lines) and measured values (points, each representing 1000 estimates) for the standard phase estimation and our implementation of Kitaev's ($M=1$) and generalized Kitaev's ($M=6$) algorithms. Error bars denote 95% confidence intervals. Our algorithm clearly has a lower standard deviation in phase estimation than both the SQL and Kitaev's algorithm (which has the SQL scaling). For large N, the curve for the adaptive algorithm is parallel to the Heisenberg limit with a small over head factor about 1.56.[8]

2.2. Quantum imaging

The techniques of preparation, control, and measurement of quantum entangled states have been developed rapidly in the last two decades, and quantum imaging has been proposed as a new field of research based on those techniques.

Ghost imaging was proposed by using the quantum correlation of twin photons from the spontaneous parametric down conversion in 1990s, which was called quantum imaging at that time. But as we known now, ghost imaging can be realized by using the classical correlation.[18,19] For example, the quantum radar based on ghost imaging is using the classical correlation of microwave. Stimulated emission depletion (STED) microscopy is a process that provides a super resolution by selectively deactivating fluorophores to enhance the imaging at a particular area, and it does not use quantum correlation or entanglement. In this review, quantum imaging is the super-resolution imaging obtained by using quantum optical fields — quantum correlation or quantum entanglement.

In 2001, Brambilla[20] analyzed the spatial aspects of quantum entanglement created in the far field of the light emitted in the spontaneous parametric down-conversion. It was found that the correlation between twin beams is much stronger than that between coherent states. And the twin entangled beams offer an opportunity to detect a weak absorption with an improved sensitivity with respect to the standard techniques which make use of the classical light sources.[21] Then they proposed a differential measurement scheme which exploits the spatial quantum correlation of type-II PDC to image a weak amplitude object with a sensitivity beyond the standard quantum limit imposed by the shot noise,[21] as shown in Fig. 8.

The measured quantity is the difference of the photon fluxes collection by the two detectors after the test beam has passed through the object, associated with the operator $N'_- = a_2^\dagger a_2 - a_1^{\dagger\prime} a_1'$, where a_1 and a_2 are the field operators of the two beams at the plane before the object. If we assume that the two beams are perfectly balanced and have symmetric statistical properties, so $\langle N_1\rangle = \langle N_2\rangle$, then we can easily obtain that the mean value of N is proportional to the object absorption coefficient $\alpha = 1 - |t_{\rm obj}|^2$

$$\langle N'_-\rangle = \langle a_2^\dagger a_2\rangle - |t_{\rm obj}|^2 \langle a_1^\dagger a_1\rangle = \langle N_1\rangle \alpha. \tag{3}$$

The noise of the measurement is determined by the variance of N'_-. The SNR of the measurement is[21]

$$\mathrm{SNR}_\sigma = \frac{N'_-}{\sqrt{\langle \delta N'^2_-\rangle}} = \frac{\alpha\sqrt{N_1}}{\sqrt{\alpha^2 E_n + 2\sigma(1-\alpha)+\alpha}}. \tag{4}$$

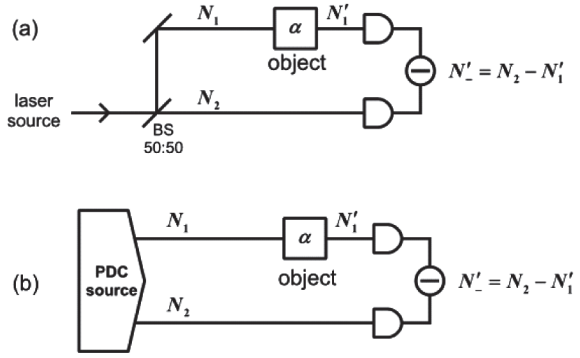


Fig. 8. Scheme for the detection of a weak object through a differential measurement. In panel (a), the test and the reference beams are obtained by splitting a laser beam with a symmetric beam splitter; in panel (b), the signal and the idler beams of a PDC source are used.[20]

In the classical scheme of Fig. 8(a), it can be verified that $\langle \delta N_-{}^2\rangle = 2\langle N_1\rangle$ whatever the amount of excess noise is.[21] Thus, we find

$$\mathrm{SNR}_{\rm class} = \frac{\alpha\sqrt{N_1}}{\sqrt{\alpha^2 E_n + 2 - \alpha}}. \tag{5}$$

If we consider the case of a coherent beam, for which $E_n = 0$, the standard quantum limit is obtained from the following expression:

$$\mathrm{SNR}_{\rm SQL} = \frac{\alpha\sqrt{N_1}}{\sqrt{2-\alpha}}. \tag{6}$$

The SQL can be beaten by using photon number correlated beams, see the scheme is Fig. 8(b). The ratio

$$R \equiv \frac{\mathrm{SNR}_\sigma}{\mathrm{SNR}_{\rm SQL}} = \sqrt{\frac{2-\alpha}{\alpha^2 E_n + 2\sigma(1-\alpha)+\alpha}} \tag{7}$$

is introduced to measures the improvement of the SNR achieved by using the PDC source with respect to the SQL. Figure 9 is the proposed scheme of high sensitivity imaging.

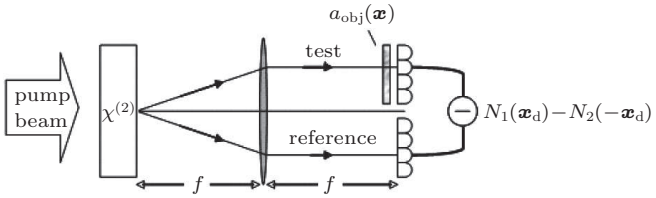


Fig. 9. High sensitivity imaging scheme that exploits subshot-noise correlations between symmetrical angular directions of a PDC field. The far field is observed in the focal plane of a lens with an f–f imaging system. The object absorption coefficient $\alpha(\boldsymbol{x})$ is retrieved by subtracting the intensities measured from the symmetrical pixels of the two arrays of detectors.[20]

In 2010, Brida *et al.*[22] presented the first experimental realization of the above scheme, showing its potential to achieve a larger signal-to-noise ratio than the classical imaging methods. They demonstrated the advantage of the subshot noise quantum imaging (SSNQI) technique over all classical imaging, including correlated imaging, when operating

at the same low illumination level. Their work represents the starting point of this quantum technology, which would have applications when there is a requirement for low-photon-flux illumination.

The works above are focused on enhancing the image contrast, and the resolution is unchanged. In the classical optical lithography, we have to use light with a short wavelength if we want to decrease the fringe separation. However with the wavelength decreased, the energy of each photon is increased. When the energy of photon is too high, the objects will be damaged. Quantum entangled states can help solve this problem. In 2000, Boto[23] proposed the quantum interferometric optical lithography. By using nonclassical photon-number states, N-photon entangled states, it is possible to write features of minimum size $\lambda/2N$ on an N-photon absorbing substrate. This result is a factor N below the classical Rayleigh diffraction limit. Subsequent works by various researchers on quantum imaging have sought to improve upon the original quantum lithography technique,[24–32] yet all of those proposals still require a multi-photon absorber as the detector[24–28,30–32] or the coincidence detection.[31] Till now, only the two-photon quantum optical lithography has been realized because of the limit of current experimental techniques.[24]

Tsang proposed a quantum imaging method, named the optical centroid measurements (OCM),[33] which can beat the Rayleigh–Abbe diffraction limit and achieve the de Broglie resolution without requiring a multi-photon absorber or the coincidence detection. By using the same nonclassical states of light as those in quantum lithography, the proposed method requires only optical intensity measurements, followed by image postprocessing, to produce the same complex quantum interference patterns as those in quantum lithography. In quantum lithography, the probability for N photons to arrive at the same place is[33]

$$\begin{aligned}\left|:\hat{I}^N(x):\right| &= \left|[\hat{A}^\dagger(x)]^N[\hat{A}(x)]^N\right| \propto \mathrm{Tr}[\hat{\Upsilon}(x,0,\ldots,0)\hat{\rho}_N] \\ &= |f(x,0,\ldots,0)|^2, \end{aligned} \tag{8}$$

which is proportional to the conditional centroid probability distribution

$$p_c(x) = \mathrm{Tr}[\hat{\Upsilon}(x,0,\ldots,0)\hat{\rho}_N]/\int \mathrm{d}x\,\mathrm{Tr}[\hat{\Upsilon}(x,0,\ldots,0)\hat{\rho}_N],$$

given that all relative positions are zero. Here $\hat{A}(x)$ is the spatial annihilation operator. The variable conjugate to the centroid position X is the total momentum $K \equiv \sum_{n=1}^{N} k_n$. The bandwidth limit on K becomes $|K \leq| 2\pi N \sin\theta/\lambda$, so the minimum feature size of the centroid distribution is on the order of $\lambda/(2N\sin\theta)$. See Fig. 10 for an illustration of the configuration-space theory.

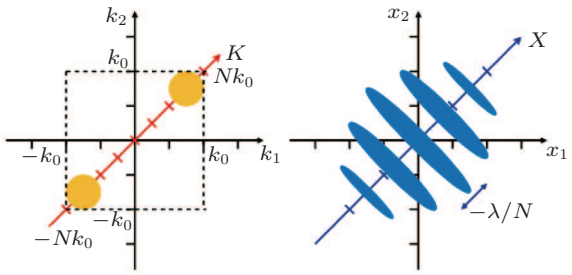


Fig. 10. Configuration-space picture of quantum imaging for $N = 2$. The Rayleigh–Abbe diffraction limit restricts the momentum wave function inside an N-dimensional box $|k_n| \leq k_0 \equiv 2\pi \sin\theta/\lambda$. The magnitude of the total momentum $K = \sum_{n=1}^{N} k_n$ is then limited by $|K| \leq Nk_0$. The minimum feature size of the wave function with respect to the centroid coordinate X is then $\sim 1/(Nk_0) \sim \lambda/N$.[33]

Despite the N-photon absorption, the intensity centroid operator can also access this centroid degree of freedom. The intensity centroid operator is

$$\hat{X} \equiv \frac{1}{N}\int \mathrm{d}x x\hat{A}^\dagger(x)\hat{A}(x), \tag{9}$$

which can be measured by spatially resolving intensity measurements, using, for example, a photon-counting detector array, followed by a calculation of the centroid of the intensity pattern, as shown schematically in Fig. 11. We can write the intensity operator as[33]

$$\begin{aligned}\hat{X} &= \hat{X}\hat{I} = \hat{X}\int \mathrm{d}x_1 \ldots \mathrm{d}x_N\, |x_1,\ldots,x_N\rangle\langle x_1,\ldots,x_N| \\ &= \int \mathrm{d}x_1 \ldots x_N \left(\frac{1}{N}\sum_{n=1}^{N} x_n\right)\prod(x_1\ldots x_N) \\ &= \int \mathrm{d}X\,\mathrm{d}\xi_1\ldots\mathrm{d}\xi_{N-1} X\hat{\Upsilon}(X,\xi_1,\ldots,\xi_{N-1}). \end{aligned} \tag{10}$$

Thus, the measurements of the intensity centroid realize the marginal positive-operator valued measure (POVM)

$$\hat{\Upsilon}(X) == \int \mathrm{d}\xi_1\ldots\mathrm{d}\xi_N \hat{\Upsilon}(X,\xi_1,\ldots,\xi_{N-1}), \tag{11}$$

and the probability distribution of the intensity centroid measurements is

$$\mathrm{Tr}[\hat{\Upsilon}(X)\hat{\rho}_N] = \int \mathrm{d}\xi_1\ldots\mathrm{d}\xi_N\, |f(X,\xi_1,\ldots,\xi_N)|^2. \tag{12}$$

This centroid marginal probability distribution also corresponds to the total momentum and has a length scale about λ/N. Besides, this marginal probability is the sum of all relative positions, much larger than that of the N-photon absorption quantum lithography. The intensity centroid measurement is illustrated in Fig. 11.

In the following year, Shin *et al.* described a variation of the OCM method with an even higher detection efficiency based on the use of photon-number-resolving detection.[34] They also reported laboratory results for the two-photon interference. Their results showed that the OCM method provides the same degree of resolution enhancement as the QL method but with higher efficiency. When large arrays of single-photon detectors become available, the OCM method would be a powerful means in providing a greater enhancement in resolution.

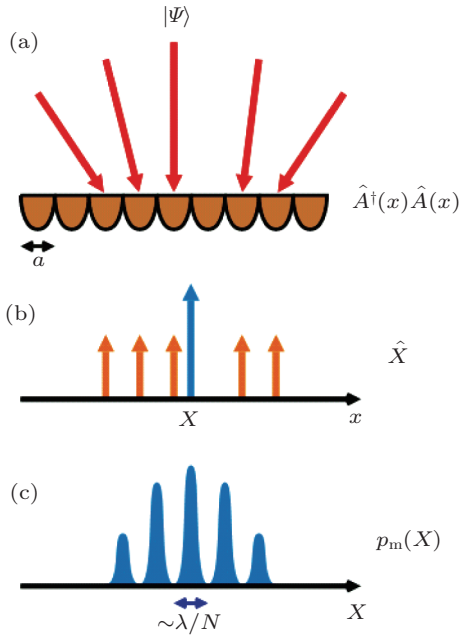


Fig. 11. (a) To measure the intensity centroid distribution, first make an ideal spatially resolving intensity measurement $[\hat{A}^{\dagger}(x)\hat{A}(x)]$, this can be done by, for example, an array of photon-counting detectors each with size $a \ll \lambda/(2\sin\theta)$. (b) The centroid X is calculated from the measured intensity pattern. (c) The intensity centroid distribution $p_{\rm m}(x)$ can then be obtained after repeated measurements of X.[33]

2.3. Precise measurement of quantum state and process

A quantum state is the carrier of quantum information and quantum computation, and a quantum process includes the preparation, control, and measurement of quantum states. To implement quantum computation and quantum information with high precision, the precise preparation, control, and measurement of quantum states are the basic requirements. The precise measurement of quantum state and process is the new research area when this new era of quantum control is coming, and new quantum techniques are needed to be developed.

2.3.1. Quantum state tomography

Measuring quantum states is always an important field in quantum mechanics. With the development of quantum information, how to measure a quantum state or a quantum process precisely becomes more and more important because we need to transport quantum information and realize quantum computation accurately. Now, quantum state tomography (QST) of maximum likelihood estimation is the most popular method for measuring a quantum state, which was proposed by James.[35] Two techniques were discussed in their work, namely, a tomographic reconstruction (in which the density matrix is linearly related to a set of measured quantities, see Fig. 11) and a maximum likelihood technique (which requires a numerical optimization but has the advantage of producing density matrices that are always non-negative definite). As Stokes showed,[35] the state of a single qubit can be determined by taking a set of four projection measurements which are represented by four operators $\hat{\mu}_0 = |H\rangle\langle H| + |V\rangle\langle V|$, $\hat{\mu}_1 = |H\rangle\langle H|$, $\hat{\mu}_2 = |D\rangle\langle D|$, and $\hat{\mu}_3 = |R\rangle\langle R|$. Similarly, the state of two qubits can be determined by a set of 16 measurements represented by operators $\hat{\mu}_i \otimes \hat{\mu}_j$ $(i,j = 0,1,2,3)$. More generally, the state of an n-qubit system can be determined with 4^n measurements given by operators $\hat{\mu}_{i_1} \otimes \hat{\mu}_{i_2} \otimes \cdots \otimes \hat{\mu}_{i_n}$ ($i_k = 0,1,2,3$ and $k = 1,2,\ldots,n$). This tree structure for multiqubit measurement is illustrated in Fig. 12. The proof of this conjecture is reasonably straight forward. The outcome of a measurement is given by the formula

$$n = N\,\mathrm{Tr}\,\hat{\rho}\hat{\mu}, \tag{13}$$

where $\hat{\rho}$ is the density matrix, $\hat{\mu}$ is the measurement operator, and N is a constant of proportionality, which can be determined from the experimental data. Thus, in the n-qubit case, the outcomes of various measurements are

$$n_{i_1,i_2,\ldots,i_n} = N\,\mathrm{Tr}\,\hat{\rho}(\hat{\mu}_{i_1} \otimes \hat{\mu}_{i_2} \otimes \cdots \otimes \hat{\mu}_{i_n}). \tag{14}$$

A likelihood function is employed to find the state with the maximum probability of obtaining the experimental data.[35] For example, for two-qubit states, the optimization problem reduces to finding the minimum of the following function:

$$L(t_1,t_2,\ldots,t_{16}) = \sum_{\nu=1}^{16} \frac{[N\langle\psi_\nu|\hat{\rho}_{\rm p}(t_1,t_2,\ldots,t_{16})|\psi_\nu\rangle - n_\nu]^2}{2N\langle\psi_\nu|\hat{\rho}_{\rm p}(t_1,t_2,\ldots,t_{16})|\psi_\nu\rangle}. \tag{15}$$

Then we can reconstruct the density matrix by inverting the parameterization of it.[35]

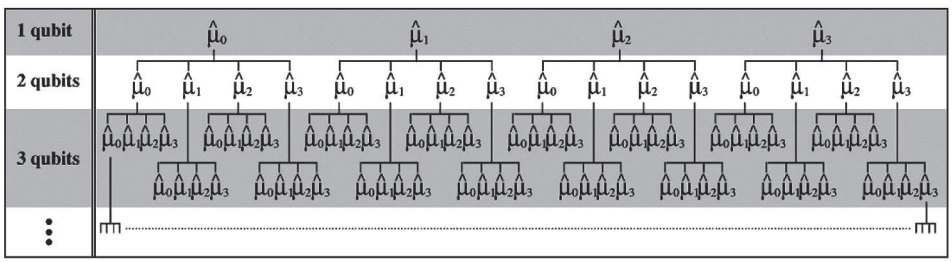


Fig. 12. Tree diagram representing numbers and types of measurements necessary for tomography. For a single qubit, the measurements $\{\hat{\mu}_0,\hat{\mu}_1,\hat{\mu}_2,\hat{\mu}_3\}$ are sufficient to reconstruct the state, e.g., measurements of the horizontal, vertical, diagonal, and right-circular polarization components. For two qubits, 16 double-coincidence measurements $\{\hat{\mu}_0\hat{\mu}_0,\hat{\mu}_0\hat{\mu}_1,\ldots,\hat{\mu}_3\hat{\mu}_3\}$ are necessary, and 64 three-coincidence measurements $\{\hat{\mu}_0\hat{\mu}_0\hat{\mu}_0,\hat{\mu}_0\hat{\mu}_0\hat{\mu}_1,\ldots,\hat{\mu}_3\hat{\mu}_3\hat{\mu}_3\}$ are necessary for three qubits, and so on.[35]

The maximum likelihood estimation (MLE)[35] is the current procedure of choice, especially for experiments. Unfortunately, it has serious flaws. It typically yields a rank-deficient estimate with one or more zero eigenvalues. Such an estimate is implausible, implying that some measurement outcomes are literally impossible.[36] No finite amount of data can justify such certainty. More importantly, it is impossible to bracket a zero probability with consistent error bars.[37] The MLE estimate is at best sub-optimal, and at worst dangerously unreliable.[36] Blume–Kohout proposed an alternative procedure,[36] the Bayesian mean estimation (BME). The BME never yields zero eigenvalues, its eigenvalues provide a bound on their own uncertainties, and under certain circumstances, it is provably the most accurate procedure possible.

The MLE and the BME are point estimates, which can never identify the state ρ or process ε exactly and are necessarily "wrong" (for instance, the matrix may have negative eigenvalues); at best, they give results close to the true state. So it is important to know how to obtain the confidence regions, that is, the regions in the state space which contain the true state with high probability.[38–40] Making rigorous and reliable statements about the system requires region estimates.[41] The confidence regions are subsets of the state space in which the true state lies in with high probability (see Fig. 13), independently of any prior assumption on the distribution of the possible states.[40–42]

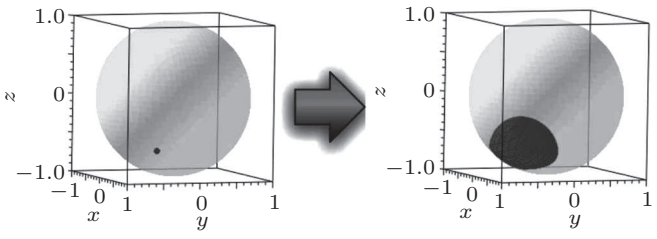


Fig. 13. Point estimators, like the maximum likelihood estimate $\hat{\rho}_{\mathrm{MLE}}$ shown on the left, cannot provide meaningful and rigorous statements about the true (but unknown) state ρ. However if we replace the point estimators with region estimators, like the likelihood-ratio confidence region shown on the right, then region $\hat{R}$ defines an assertion — ρ lies within $\hat{R}$ with 90% certainty — that is rigorously valid. The estimates shown here come from simulated measurements on 60 copies of a single-qubit state, with 20 measurements each of σ_x, σ_y, and σ_z yielding $+/-$ counts of $7/13$, $9/11$, and $3/17$, respectively.[41]

At the same time, the MLE and the BME are optimal when the quantum resources are infinite, however most of time, the quantum resources are finite. Recently, scientists are working on how to improve the precision with finite resources.[43–49] Adaptive quantum state tomography can help enhance the precision. If N denotes the number of measurement trials and N is sufficiently large, it is known in the 1-qubit state estimation that the expectation value of infidelity averaged over states, a measure of the estimation error, can decrease at best $\mathrm{O}(N^{-3/4})$ in a nonadaptive experiment,[50] compared to $\mathrm{O}(N^{-1})$ in the adaptive experiments,[46] as shown in Fig. 14.

2.3.2. Quantum process tomography

Quantum process tomography (QPT) deals with identifying an unknown quantum dynamical process. There are two ways for quantum process tomography. One is using the known quantum states to probe a quantum process and find out how the process can be described by quantum state tomography.[37,51–55] The first approach, introduced in 1996 and sometimes known as the standard quantum process tomography (SQPT), involves preparing an ensemble of quantum states, sending them through the process, and then using quantum state tomography to identify the resultant states.[51] Other techniques include ancilla-assisted process tomography (AAPT) and entanglement-assisted process tomography (EAPT), which require an extra copy of the system.[37]

All the techniques listed above are known as indirect methods for the characterization of quantum process, since they require the use of quantum state tomography to reconstruct the quantum process. In contrast, there are direct methods, such as the direct characterization of quantum dynamics (DCQD), which provide a full characterization of quantum systems without any state tomography.[56–60]

With the development of quantum techniques, quantum states with more and more qubits can be prepared. A fundamental difficulty in demonstrating quantum state (process) tomography is that the required resources grow exponentially with the system size. Now, it is research hotspots to reduce the measurement bases and time for data analysis processes.[49,61–65] Cramer *et al.* presented two tomography schemes that scale much more favorably with system size than the direct tomography.[61] one of them requires unitary operations on a constant number of subsystems, whereas the other requires only local measurements together with more elaborate post-processing. Both rely only on a linear number of experimental operations and post-processing that is polynomial in the system size. Recently, scientists adopt techniques from compressive sensing to develop experimentally efficient methods for QST and QPT[63,64] and proposed a technique for performing quantum state tomography on multiple-qubit states despite the incomplete knowledge about the unitary operations used to change the measurement basis, named the self-calibrating quantum state tomography.[65]

Beside the above research areas, quantum metrology has many other branches, such as quantum optical coherent tomography,[66–68] quantum positioning and clock synchronization,[69–72] and quantum radar.[73–75]

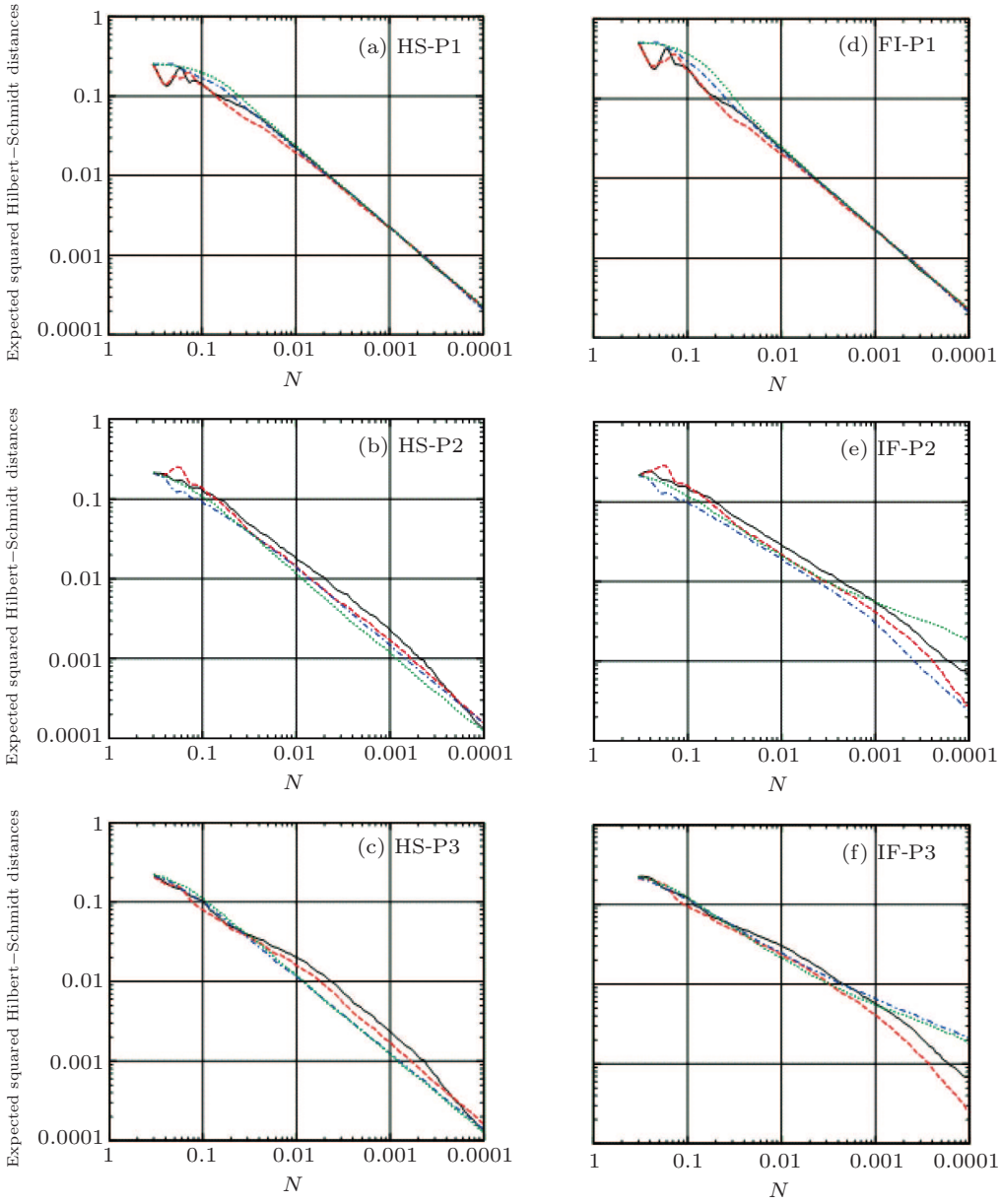


Fig. 14. Point wise expected loss $\bar{\Delta}_N(u^N, \boldsymbol{s}^{\rm est}|\boldsymbol{s})$ against the number of trials N (the horizontal and vertical axes are both in logarithmic scale): (a) HS-P1, (b) HS-P2, and (c) HS-P3 are the expected squared Hilbert–Schmidt distances for $\boldsymbol{s}$ given by $(r,\theta,\phi) = (0,0,0),(0.99,0,0),(0.99,4,4)$, and (d) IF-P1, (e) IF-P2, and (f) IF-P3 are the expected infidelities for the same three true states, respectively. The number of measurement trials, $N_{\rm max}$, is 10000, and the number of sequences used for the calculation of statistical expectation values, $N_{\rm mean}$, is 1000.[46]

3. Conclusion and perspectives

Quantum metrology is the study of making high-resolution and highly-sensitive measurements of physical parameters, classical and quantum parameters, using quantum theory to describe the physical systems, particularly exploiting the quantum entanglement and quantum squeezed states.

With great improvements in controlling quantum systems, quantum metrology has attracted a lively interest in recent years and great achievements have been gained, as shown in this paper. It is demonstrated that quantum metrology can give better precision than the same measurement performed in a classical framework when consuming commensurable resources. This means that quantum metrology can use less resources and obtain more precise measurements. However because of the limit of quantum techniques, quantum metrology is at the early research stage, plenty of theoretical and experimental techniques need to be developed, such as the technique of quantum state preparation, especially for multi-qubit states, high efficiency quantum measurement methods, and high precision quantum measurement techniques. These are the impassable science problems in the development of quantum metrology.

In conclusion, we anticipate that quantum metrology will be broadly used in near future and it will promote the development of quantum information sciences, both theoretically

and experimentally, because it has higher precision than the classical metrology and the quantum parameters can only be measured by quantum metrology.

References

[1] Einstein A, Podolsky B and Rosen N 1935 *Phys. Rev.* **47** 777
[2] Giovannetti V, Lloyd S and Maccone L 2004 *Science* **306** 1330
[3] Xiao M, Wu L A and Kimble H J 1987 *Phys. Rev. Lett.* **59** 278
[4] Nagata T, Okamoto R, O'Brien J L, Sasaki K and Takeuchi S 2007 *Science* **316** 726
[5] Holland M J and Burnett K 1993 *Phys. Rev. Lett.* **71** 1355
[6] Sun F W, Liu B H and Huang Y F 2008 *Europhys. Lett.* **82** 24001
[7] Xiang G Y, Hofmann H F and Pryde G J 2013 *Scientific Reports* **3** 2684
[8] Higgins B L, Berry D W, Bartlett S D, Wiseman H M and Pryde G J 2007 *Nature* **450** 393
[9] Xiang G Y, Higgins B L, Berry D W, Wiseman H M and Pryde G J 2011 *Nature Photonics* **5** 43
[10] Okamoto R, Hofmann H F, Nagata T, O'BrienJ L, Sasaki K and Takeuchi S 2008 *New J. Phys.* **10** 073033
[11] Crespi A, Lobino M, Matthews J C F, Politi A, Neal C R, Ramponi R, Osellame R and O'Brien J L 2012 *Appl. Phys. Lett.* **100** 233704
[12] The LIGO Scientific Collaboration 2011 *Nature Phys.* **7** 962
[13] Huver S D, Wildfeuer C F and Dowling J P 2008 *Phys. Rev. A* **78** 063828
[14] Kacprowicz M, Demkowicz-Dobrzanski R, Wasilewski W, Banaszek K and Walmsley I A 2010 *Nature Photonics* **4** 357
[15] Escher B M, de Matos Filho R L and Davidovich L 2011 *Nature Phys.* **7** 406
[16] Hall M J W, Berry D W, Zwierz M and Wiseman H M 2011 arXiv:1111.0788
[17] Yonezawa H, Nakane D, Wheatley T A, Iwasawa K, Takeda S, Arao H, Ohki K, Tsumura K, Berry D W, Ralph T C, Wiseman H M, Huntington E H and Furusawa A 2012 *Science* **337** 1514
[18] Gatti A, Brambilla E, Bache M and Lugiato L A 2004 *Phys. Rev. A* **70** 013802
[19] Gatti A, Brambilla E, Bache M and Lugiato L A 2004 *Phys. Rev. Lett.* **93** 093602
[20] Brambilla E, Gatti A, Lugiato L A and Kolobov M I 2001 *Eur. Phys. J. D* **15** 127
[21] Brambilla E, Caspani L, Jedrkiewicz O, Lugiato L A and Gatti A 2008 *Phys. Rev. A* **77** 053807
[22] Brida G, Genovese M and Ruo Berchera I 2010 *Nature Photonics* **4** 227
[23] Boto N, Kok P, Abrams D S, Braunstein S L, Williams C P and Dowling J P 2000 *Phys. Rev. Lett.* **85** 2733
[24] Angelo M D, Chekhova M V and Shih Y H 2001 *Phys. Rev. Lett.* **87** 013602
[25] Agarwaletal G S 2001 *Phys. Rev. Lett.* **86** 1389
[26] Bentley S J and Boyd R W 2004 *Opt. Express* **12** 5735
[27] Boyd R W and Bentley S J 2006 *J. Mod. Opt.* **53** 713
[28] Hemmer P R 2006 *Phys. Rev. Lett.* **96** 163603
[29] Bjork G, Sanchez-Soto L L and Soderholm J 2001 *Phys. Rev. Lett.* **86** 4516
[30] Bjork G, Sanchez-Soto L L and Soderholm J 2001 *Phys. Rev. A* **64** 013811
[31] Thiel C, Bastin T, Martin J, Solano E, von Zanthier J and Agarwal G S 2007 *Phys. Rev. Lett.* **99** 133603
[32] Giovannetti V, Lloyd S, Maccone L and Shapiro J H 2009 *Phys. Rev. A* **79** 013827
[33] Tsang M 2009 *Phys. Rev. Lett.* **102** 253601
[34] Shin H, Chan K W C, Chang H J and Boyd R W 2011 *Phys. Rev. Lett.* **107** 083603
[35] James D F V, Kwiat P G, Munro W J and White A G 2001 *Phys. Rev. A* **64** 052312
[36] Blume-Kohout R 2010 *New J. Phys.* **12** 043034
[37] Altepeter J B, Branning D, Jeffrey E, Wei T C, Kwiat P G, Thew R T, O'Brien J L, Nielsen M A and White A G 2003 *Phys. Rev. Lett.* **90** 193601
[38] Blume-Kohout R, Yin J O S and van Enk S J 2010 *Phys. Rev. Lett.* **105** 170501
[39] Yin J O S and van Enk S J 2011 *Phys. Rev. A* **83** 062110
[40] Gross D, Liu Y K, Flammia S T, Becker S and Eisert J 2010 *Phys. Rev. Lett.* **105** 150401
[41] Blume-Kohout R 2012 arXiv:1202.5270
[42] Christandl M and Renner R 2012 *Phys. Rev. Lett.* **109** 120403
[43] Adamson R B A and Steinberg A M 2010 *Phys. Rev. Lett.* **105** 030406
[44] Tóth G, Wieczorek W, Gross D, Krischek R, Schwemmer C and Weinfurter H 2010 *Phys. Rev. Lett.* **105** 250403
[45] Huszar F and Houlsby N M T 2012 *Phys. Rev. A* **85** 052120
[46] Sugiyama T, Turner P S and Murao M 2012 *Phys. Rev. A* **85** 052107
[47] Kravtsov K S, Straupe S S, Radchenko I V, Houlsby N M T and Kulik S P 2013 arXiv:1303.1792
[48] Mahler D H, Rozema L A, Darabi A, Ferrie C, Blume-Kohout R and Steinberg A M 2013 arXiv:1303.0436
[49] Qi B, Hou Z B, Li L, Dong D Y, Xiang G Y and Guo G C 2013 arXiv:1304.6827
[50] Bagan E, Baig M, Munoz-Tapia R and Rodriguez A 2004 *Phys. Rev. A* **69** 010304
[51] Chuang I L and Nielsen M A 1996 arXiv:quant-ph/9610001
[52] Nielsen M A and Chuang I L 2000 *Quantum Computation and Quantum Information* (Cambridge: Cambridge University Press)
[53] Chuang I L and Nielsen M A 1997 *J. Mod. Opt.* **44** 2455
[54] Poyatos J F, Cirac J I and Zoller P 1997 *Phys. Rev. Lett.* **78** 390
[55] Anis A and Lvovsky A I 2012 *New J. Phys.* **14** 105021
[56] Leung D W 2003 *J. Math. Phys.* **44** 528
[57] D'Ariano G M and Lo Presti P 2001 *Phys. Rev. Lett.* **86** 4195
[58] D'Ariano G M and Lo Presti P 2003 *Phys. Rev. Lett.* **91** 047902
[59] da Silva M P, Landon-Cardinal O and Poulin D 2011 *Phys. Rev. Lett.* **107** 210404
[60] Graham T M, Barreiro J T, Mohseni M and Kwiat P G 2013 *Phys. Rev. Lett.* **110** 060404
[61] Cramer M, Plenio M B, Flammia S T, somma R, Gross D, Bartlett S D, Landon-Cardinal O, Poulin D and Liu Y K 2010 *Nat. Commu.* **1** 149
[62] Smolin J A, Gambetta J M and Smith G 2012 *Phys. Rev. Lett.* **108** 070502
[63] Shabani A, Kosut R L, Mohseni M, Rabitz H, Broome M A, Almeida M P, Fedrizzi A and White A G 2011 *Phys. Rev. Lett.* **106** 100401
[64] Liu W T, Zhang T, Liu J Y, Chen P X and Yuan J M 2012 *Phys. Rev. Lett.* **108** 170403
[65] Branczyk A M, Mahler D H, Rozema L A, ADarabi, Steinberg A M and James D F V 2012 *New J. Phys.* **14** 085003
[66] Abouraddy A F, Nasr M B, Saleh B E A, Sergienko A V and Teich M C 2002 *Phys. Rev. A* **65** 053817
[67] Nasr M B, Saleh B E A, Sergienko A V and Teich M C 2003 *Phys. Rev. Lett.* **91** 083601
[68] Lopez-Mago D and Novotny L 2012 *Opt. Lett.* **37** 4077
[69] Giovannetti V, Lloyd S and Maccone L 2001 *Nature* **412** 417
[70] Bahder T B 2004 quant-ph/0406126
[71] Giovannetti V, Lloyd S and Maccone L 2002 *Phys. Rev. A* **65** 022309
[72] Valencia A, Scarcelli G and Shih Y H 2004 *Appl. Phys. Lett.* **85** 2655
[73] Nagy G A 2011 arxiv:1101.2223
[74] http://www.dtic.mil/cgi-bin/GetTRDoc?AD=ADA502521
[75] http://www.dtic.mil/cgi-bin/GetTRDoc?AD=ADA506209